

FIRST-PRINCIPLES STUDY OF THERMODYNAMIC STABILITY AND ELASTICITY OF La5Ni19

¹Martin FRIÁK, ^{1,2}Sabina KOVAŘÍKOVÁ OWEIS, ^{2,1}Jana PAVLŮ, ³David HOLEC, ¹Ondřej ZOBAČ, ⁴Monika KAWULOKOVÁ, ⁴Simona ZLÁ, ⁴Bedřich SMETANA

¹Institute of Physics of Materials, v.v.i., Czech Academy of Sciences, Žižkova 22, Brno, 616 00, Czech Republic, EU, <u>friak@ipm.cz</u>, <u>kovarikova@ipm.cz</u>, <u>zobac@ipm.cz</u>

²Department of Chemistry, Faculty of Science, Masaryk University, Kotlářská 2, Brno, 611 37, Czech Republic, EU, <u>houserova@chemi.muni.cz</u>

³Department of Materials Science, Technical University of Leoben, Franz-Josef-Straße 18, Leoben, A-8700, Austria, EU, <u>david.holec@unileoben.ac.at</u>

⁴Department of Chemistry and Physico-Chemical Processes, Faculty of Materials Science and Technology, VSB Technical University of Ostrava, 17. listopadu 15, Ostrava, 708 00, Czech Republic, EU, monika.kawulokova@vsb.cz, simona.zla@vsb.cz, bedrich.smetana@vsb.cz

https://doi.org/10.37904/metal.2025.5092

Abstract

La-Ni compounds are considered promising candidates for future hydrogen-storage applications. Some of the La-Ni phases have been insufficiently studied so far and some critically important data are missing. In particular, the La₅Ni₁₉ intermetallic compound is reported to crystallize in either hexagonal or trigonal R3 phase, but the stability of these two variants has not been satisfactorily addressed. We have employed quantum-mechanical calculations implementing the density functional theory within the generalized gradient approximation to determine the ground-state structural, electronic, magnetic, thermodynamic, and elastic properties of the two phases. The hexagonal phase is described by a computational cell containing 48 atoms, while the trigonal phase contains 72 atoms. Both computational cells are strongly anisotropic. Static lattice calculations indicate that both phases are very similar with the hexagonal phase having a slightly lower formation energy (by less than 1 meV/atom). The computational cell volumes and the total magnetic moments are practically identical in both phases. Further, the stress-strain method proved (by computing a full tensor of the second-order elastic constants) that both phases are mechanically stable.

Keywords: La-Ni, quantum-mechanical calculations, stability, thermodynamics, elasticity

1. INTRODUCTION

Effective energy storage remains a critical obstacle in the full-scale transition to renewable energy sources, with hydrogen storage standing out as a particularly promising technology. Metal hydrides represent a viable class of materials for this application, offering high volumetric hydrogen density and advantageous safety features. Nevertheless, ongoing research is necessary to identify compositions that balance high hydrogen storage capacity and suitable absorption/desorption kinetics at practical operating temperatures. Binary La-Ni materials derived from LaNi₅ exhibit noteworthy structural and electronic characteristics, particularly relevant for hydrogen storage and other energy-related technologies [1, 2]. The properties of these materials can be systematically tailored through alloying, specifically by partially substituting individual atomic species [3]. Such modifications can significantly alter the crystal structure and lattice parameters, thereby playing a crucial role in determining hydrogen absorption behavior [4].

Our study of two modifications of the La₅Ni₁₉ compound was motivated by the limited understanding of the stability of phases in the La-Ni system. This lack of data negatively affects the development of suitable storage-



related hydrides. We focus on the hexagonal and trigonal La₅Ni₁₉ phase and employ a quantum-mechanical approach to explore their equilibrium characteristics, electronic structure as well as their thermodynamic and mechanical (elastic) stability.

2. COMPUTATIONAL METHODOLOGY

Our first-principles calculations were performed using the Vienna Ab initio Simulation package (VASP) [5,6] within the Density Functional Theory (DFT) [7,8] employing Projector Augmented Wave (PAW) [9,10] pseudopotentials (an 11-valence-electron La potential and a 16-valence-electron Ni_pv potentials from the potpaw_PBE.52 VASP database). The exchange-correlation energy was approximated by the Generalized Gradient Approximation (GGA) as parametrized by Perdew, Burke and Ernzerhof (PBE'96) [11]. The planewave energy cut-off was 520 eV. We used the Methfessel-Paxton smearing scheme of order 1 with the smearing parameter set to 0.1. The reciprocal-space Brillouin zone of the 48-atom hexagonal La₅Ni₁₉ (**Figure 1(b)**) by a 10×10×1 k-point mesh. Single-crystal elastic constants were computed by the stress-strain method [12].

3. RESULTS

Our calculations started with a full structural relaxation of both phases, i.e., the minimization of the energy of the static lattices with respect to the atomic positions as well as the computational-cell shape and volume. The resulting minimum-energy lattice parameters are equal to a = b = 0.5009 nm and c = 3.2558 nm for the hexagonal phase and a = b = 0.5009 nm and c = 4.8837 nm for the trigonal phase. In the trigonal phase, the a and b lattice parameters are equal, consistent with the hexagonal-shape of its unit cell. The lattice parameters a = b are also practically identical in both phases. Both phases are magnetic, with the total magnetic moments equal to 3.22 μ_B and 3.26 μ_B per 24-atom (one half of 48-atom hexagonal cell and one third of the 72-atom trigonal cell) formula unit for the hexagonal and trigonal phases, respectively.

The thermodynamic stability of the two studied phases of La₅Ni₁₉ was assessed by evaluating their formation energy ΔE_f . Its mathematical expression is specifically for La₅Ni₁₉ as follows:

$$\Delta E_f(\text{La}_5\text{Ni}_{19}) = \frac{E(\text{La}_5\text{Ni}_{19}) - 5 * E(\text{La}) - 19 * E(\text{Ni})}{5 + 19},$$

where we used the static-lattice energy $E(\text{La}_5\text{Ni}_{19})$ of the $\text{La}_5\text{Ni}_{19}$ and energies of constituting pure elements in their ground-state structures, in particular, E(La) for the non-magnetic hexagonal close-packed (hcp) La and E(Ni) for the ferromagnetic face-centred-cubic (fcc) Ni.

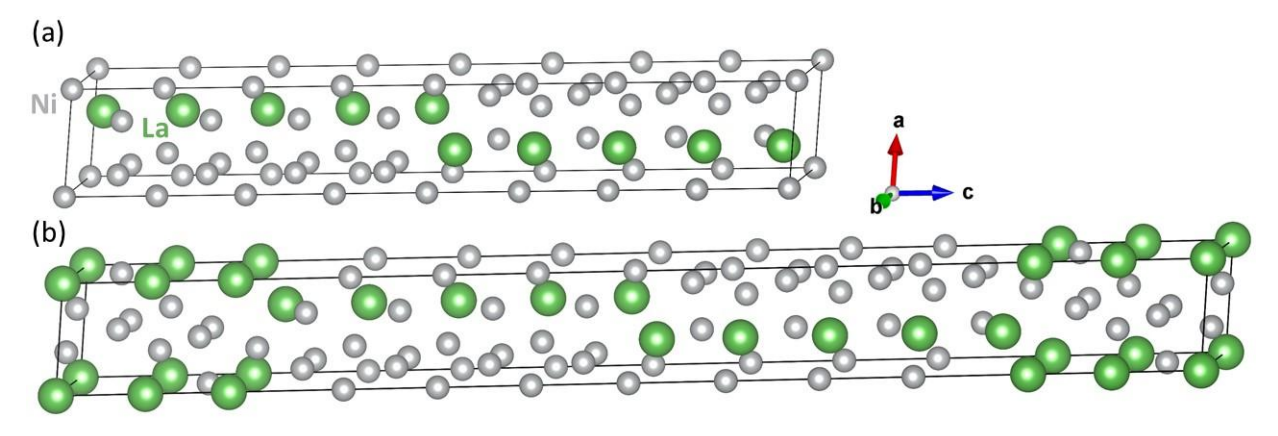


Figure 1 Visualizations of the computed variants of La₅Ni₁₉,(a) 48-atom hexagonal phase and (b) 72-atom trigonal R3 phase



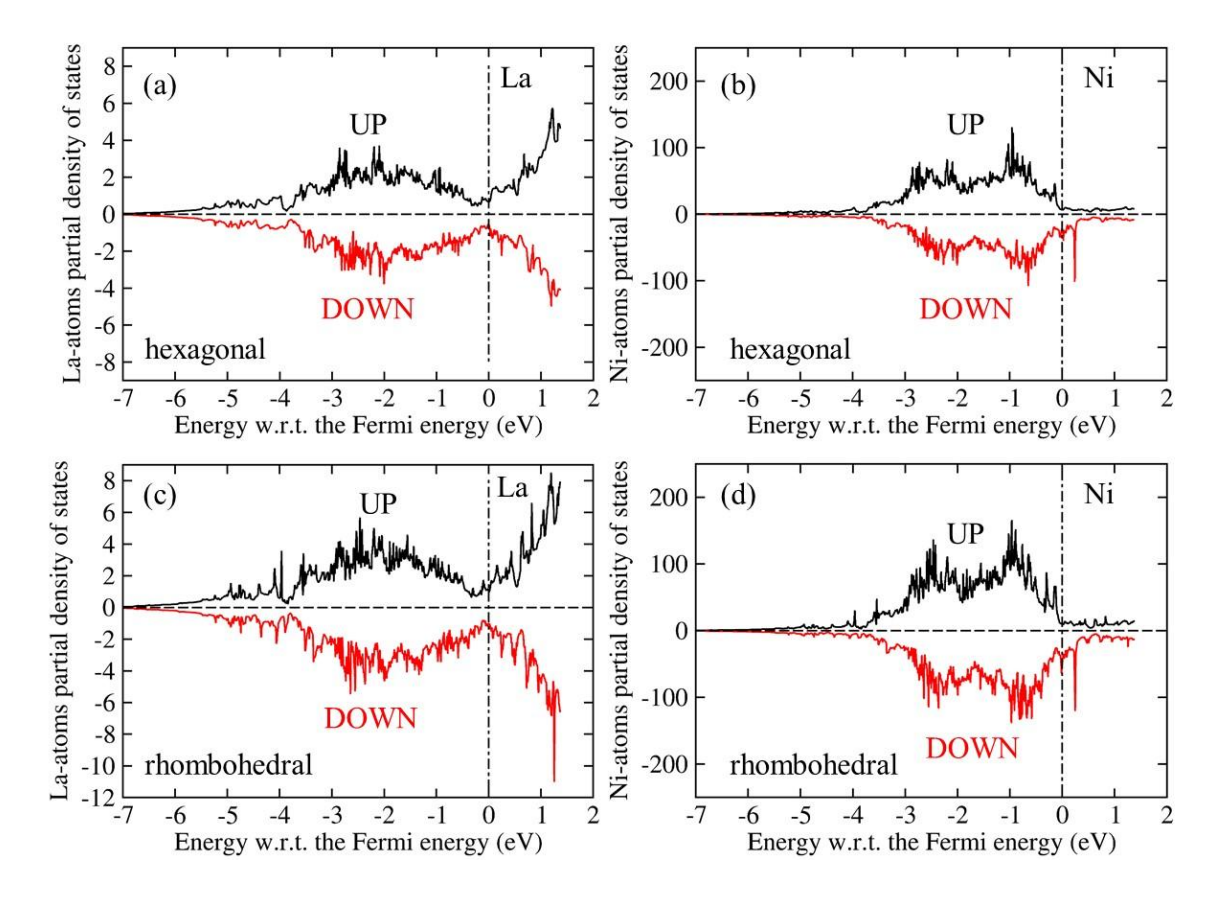


Figure 2 Computed UP/DOWN density of electronic states of the hexagonal (a,b) and trigonal (c,d) La₅Ni₁₉ projected on the La atoms (a,c) and the Ni atoms (b,d)

The computed formation energies are equal to -0.3082 meV/atom and -0.3079 meV/atom for the hexagonal and trigonal phase, respectively. We conclude that the studied phases have very similar thermodynamic stabilities and as the formation energy is negative, both phases are stable with respect to the decomposition into the elemental La and Ni.

The electronic structure is presented in the form of partial densities of electronic states separately for the La and Ni atoms for both phases in **Figure 2**. Both materials are metals with non-zero density of states at the Fermi level. Further, the electronic band structure of the hexagonal and trigonal phase is shown in **Figure 3** and **4**, respectively. Interestingly, bands for both spin channels are very similar.

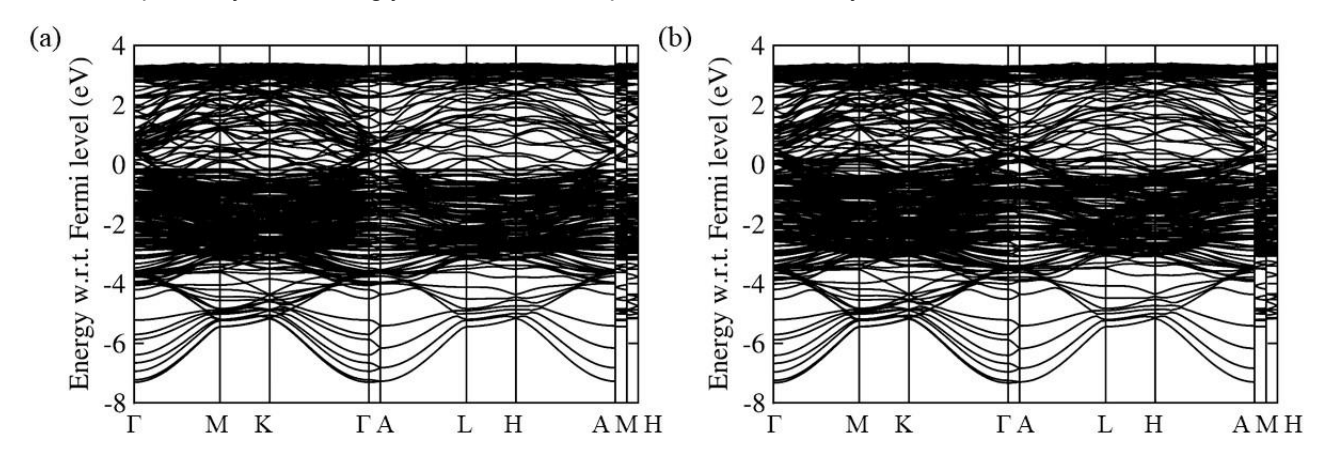


Figure 3 The computed electronic band structure of the hexagonal variant of La₅Ni₁9, for the UP spin density (a) and DOWN spin density (b)



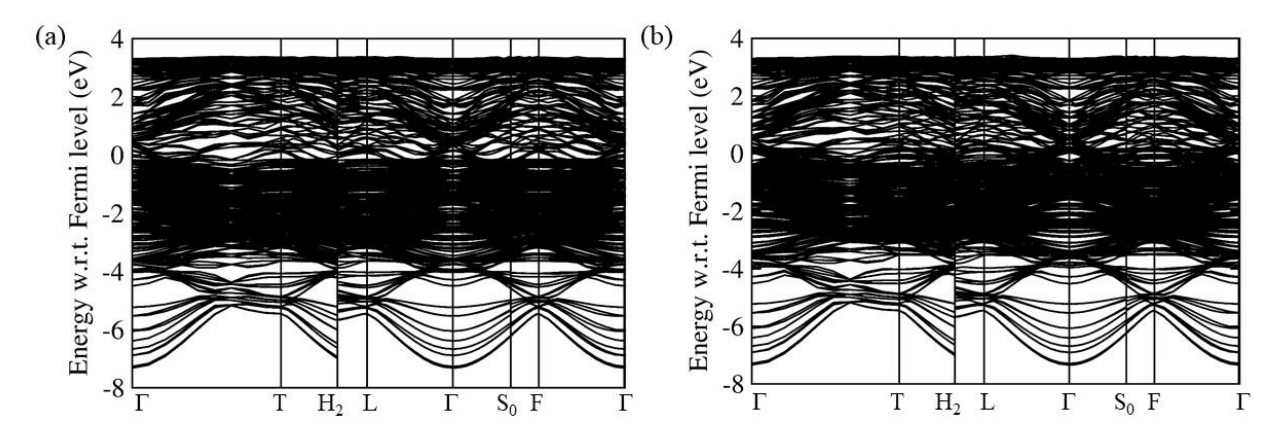


Figure 4 The computed electronic band structure of the trigonal La₅Ni₁₉, for the UP spin density (a) and DOWN spin density (b)

Our next step was examining the mechanical stability and elastic properties of both studied phases of La₅Ni₁₉. We have determined a full tensor of their elastic constants. As our calculations have an error-bar of a few GPa and these errors artificially reduced the symmetry of the tensor, we projected [13] these two computed tensors of elastic constants onto tensors with a hexagonal and trigonal symmetry, respectively. We present the computed elastic constants (in GPa) as 6×6 matrices for the hexagonal (left) and trigonal (right) phases:

| 191 | 108 | 88 | 0 | 0 | 0 | 182 | 118 | 90 | 0 | 0 | 0 |
|-----|-----|-----|----|----|----|-----|-----|-----|----|----|----|
| 108 | 191 | 88 | 0 | 0 | 0 | 118 | 182 | 90 | 0 | 0 | 0 |
| 88 | 88 | 211 | 0 | 0 | 0 | 90 | 90 | 212 | 0 | 0 | 0 |
| 0 | 0 | 0 | 51 | 0 | 0 | 0 | 0 | 0 | 51 | 0 | 0 |
| 0 | 0 | 0 | 0 | 51 | 0 | 0 | 0 | 0 | 0 | 51 | 0 |
| 0 | 0 | 0 | 0 | 0 | 42 | 0 | 0 | 0 | 0 | 0 | 42 |

The computed single-crystal elastic properties of both phases are visualized in the form of directional dependences of Young's modulus in **Figure 5**.

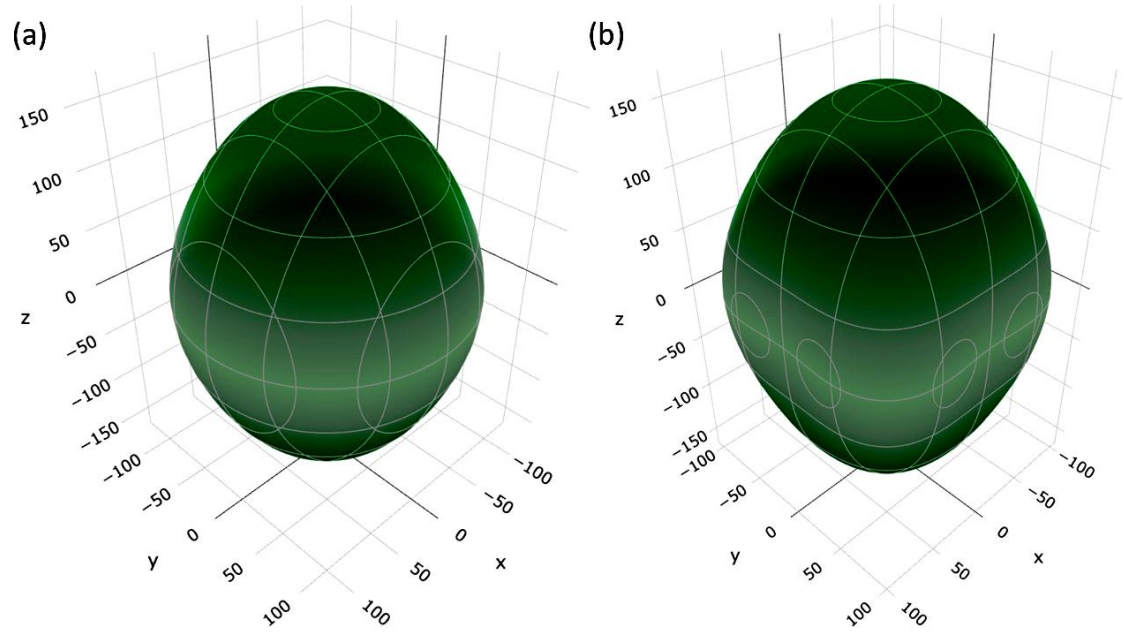


Figure 5 Computed directional dependences of single-crystal Young's modulus (in GPa) of La₅Ni₁₉ in (a) the hexagonal phase and (b) the trigonal phase. The visualization was done by the ELATE [14]



Table 1 Homogenized elastic characteristics (bulk modulus, Young's modulus, shear modulus and Poisson's ratio) according to Voigt's, Reuss' and Hill's homogenization methods for both the hexagonal and trigonal phase (values for the trigonal phase are in parentheses) as evaluated by the ELATE software tool [14] (openaccess online at https://progs.coudert.name/elate).

| Homogenization method | Bulk modulus (GPa) | Young's modulus (GPa) | Shear modulus (GPa) | Poisson's ratio (-) |
|-----------------------|-----------------------|--------------------------|------------------------|---------------------|
| Voigt | 129 (130) | 131 (132) | 49 (50) | 0.3302 (0.3310) |
| Reuss | 129 (130) | 129 (128) | 48 (48) | 0.3338 (0.3354) |
| Hill | 129 (130) | 130 (130) | 49 (49) | 0.3318 (0.3332) |

As shown in **Figure 5**, both studied phases of La₅Ni₁₉ are only weakly elastically anisotropic despite of their highly anisotropic unit cells, see **Figure 1** above. Regarding the mechanical stability, a system is considered mechanically stable if all the eigenvalues of its 6x6 matrix of the single-crystal elastic constants are positive. We used the ELATE software to determine these eigenvalues for both structures and we got the following eigenvalues: 42, 51, 51, 83, 123, 387 (all in GPa) for the hexagonal phase and 42, 51, 51, 64, 121, 391 (all in GPa) for the trigonal phase. As they are all positive, both variants of La₅Ni₁₉ are computed mechanically stable.

Lastly, using the ELATE software [14], we also determined homogenized polycrystal characteristics (bulk modulus, Young's modulus, shear modulus and Poisson's ratio) from single-crystal elastic constants according to three homogenization methods (Voigt, Reuss, Hill). Their values are listed for both phases in Table T1. Again, both phases have turned out to have very similar elastic characteristics.

4. CONCLUSION

Motivated by the lack of data related to several phases from the La-Ni system, we employed quantum-mechanical calculations to assess the thermodynamic and elastic stability of La $_5$ Ni $_{19}$ intermetallic compound in its hexagonal and trigonal variants. We determined the minimum-energy static-lattice structural, electronic, magnetic, thermodynamic, and elastic properties. Both computed phases have very similar formation energies (-0.3082 meV/atom and -0.3079 meV/atom for the hexagonal and trigonal phase, respectively) and are stable with respect to the decomposition into the elemental La and Ni. Regarding structural characteristics, the a=b lattice parameters are practically identical in both phases. The total magnetic moments per 24-atom formula unit are very similar, too, equal to 3.22 μ_B and 3.26 μ_B for the hexagonal and trigonal phase, respectively. Further, we employed the stress-strain method to address the mechanical stability by computing a full tensor of the second-order elastic constants. Both phases are elastically only weakly anisotropic and our analysis of the eigenvalues of the 6×6 matrices of single-crystal elastic constants revealed that all eigenvalues are positive and, therefore, both studied phases are mechanically stable.

ACKNOWLEDGEMENTS

This study was created as part of the project No. CZ.02.01.01/00/22_008/0004631 Materials and technologies for sustainable development within the Jan Amos Komensky Operational Program financed by the European Union and from the state budget of the Czech Republic. Computational resources were made available by the Ministry of Education, Youth and Sports of the Czech Republic under the Project e-INFRA CZ (ID:90254) at the IT4Innovations National Supercomputing Center, the MetaCentrum and CERIT-SC. Access to the CERIT-SC computing and storage facilities provided by the CERIT-SC Center, under the programme "Projects of Large Research, Development, and Innovations Infrastructures" (CERIT Scientific Cloud LM2015085) and access to CESNET storage facilities provided by the project "e-INFRA CZ" under the programme "Projects of Large Research, Development, and Innovations Infrastructures" LM2023054) is acknowledged. The computational



cells in Figure 1 were visualized using the VESTA package [15]. We also acknowledge the use of the VASPKIT software package [16,17].

DATA AVAILABILITY

The VASP files of the hexagonal La_5Ni_{19} are available at DOI: 10.5281/zenodo.15395882 The VASP files of the trigonal La_5Ni_{19} are available at DOI: 10.5281/zenodo.15395914

REFERENCES

- [1] GIZA, K., IWASIECZKO, W., PAVLYUK, V. V., BALA, H., DRULIS, H. Thermodynamical properties of La–Ni–T (T = Mg, Bi and Sb) hydrogen storage systems. *J. Power Sources*. 2008, vol. 181, no. 1, pp. 38–40. DOI: 10.1016/j.jpowsour.2007.12.018.
- [2] JOUBERT, J.-M., PAUL-BONCOUR, V., CUEVAS, F., ZHANG, J., LATROCHE, M. LaNi₅ related AB₅ compounds: Structure, properties and applications. *J. Alloys Compd.* 2021, vol. 862, pp. 158163. DOI: 10.1016/j.jallcom.2020.158163.
- [3] MI, W., LIU, Z., KIMURA, T., et al. Crystal structure and hydrogen storage properties of (La,Ce)Ni₅-xM_x (M = Al, Fe, or Co) alloys. *Int. J. Miner. Metall. Mater.* 2019, vol. 26, pp. 108–113. DOI: 10.1007/s12613-019-1714-z.
- [4] VALØEN, L. O., ZALUSKA, A., ZALUSKI, L., TANAKA, H., KURIYAMA, N., STRÖM-OLSEN, J. O., TUNOLD, R. Structure and related properties of (La,Ce,Nd,Pr)Ni₅ alloys. *J. Alloys Compd.* 2000, vol. 306, nos. 1–2, pp. 235–244. DOI: 10.1016/S0925-8388(00)00765-9.
- [5] KRESSE, G., HAFNER, J. Ab initio molecular dynamics for liquid metals. *Physical Review B.* 1996, vol. 47, p. 558. https://doi.org/10.1103/PhysRevB.47.558.
- [6] KRESSE, G., FURTHMÜLLER, J. Efficient iterative schemes for ab initio total energy calculations using a plane-wave basis set. *Physical Review B*. 1996, vol. 54, p. 11169. https://doi.org/10.1103/PhysRevB.54.11169.
- [7] HOHENBERG, P., KOHN, W. Inhomogeneous electron gas. *Physical Review B*, 1964, vol. 136, p. B864. https://doi.org/10.1103/PhysRev.136.B864.
- [8] KOHN, W., SHAM, L. J. Self-consistent equations including exchange and correlation effects. *Physical Review A.* 1965, vol. 140, pp. A1133. https://doi.org/10.1103/PhysRev.140.A1133.
- [9] BLÖCHL, P. E. Projector augmented-wave method. *Physical Review B.* 1994, vol. 50, p. 17953. https://doi.org/10.1103/PhysRevB.50.17953.
- [10] KRESSE, G., JOUBERT, D. From ultrasoft pseudopotentials to the projector augmented-wave method. *Physical Review B.* 1999, vol. 59, p. 1758. https://doi.org/10.1103/PhysRevB.59.1758.
- [11] PERDEW, J. P., BURKE, K., ERNZERHOF, M. Generalized gradient approximation made simple. *Physical Review Letters*. 1996, vol. 77, pp. 3865. https://doi.org/10.1103/PhysRevLett.77.3865.
- [12] ZHOU, L., HOLEC, D., MAYRHOFER, P.H. Alloying-related trends from first principles: An application to the Ti-Al-X-N system. *Journal of Applied Physics*. 2013, vol. 113, p. 113510. https://doi.org/10.1063/1.4795590.
- [13] MOAKHER, M., NORRIS, A. N. The closest elastic tensor of arbitrary symmetry to an elasticity tensor of lower symmetry. *Journal of Elasticity*. 2004, vol. 85, pp. 215–263.
- [14] GAILLAC, R., et al., ELATE: an open-source online application for analysis and visualization of elastic tensors. *J. Phys.: Condens. Matter.* 2016, vol. 28, p. 275201. DOI <u>10.1088/0953-8984/28/27/275201</u>.
- [15] MOMMA, K., IZUMI, F. VESTA 3 for three-dimensional visualization of crystal, volumetric and morphology data. *Journal of Applied Crystalography*. 2006, vol. 44, p. 1272. https://doi.org/10.1107/S0021889811038970.
- [16] WANG, V., XU, N., LIU, J.-C., TANG, G. GENG, W.-T, VASPKIT: A user-friendly interface facilitating high-throughput computing and analysis using VASP code. *Computer Physics Communications*. 2021, vol. 267, p. 108033. DOI: 10.1016/j.cpc.2021.108033.
- [17] HINUMA, Y., PIZZI, G., KUMAGAI, Y., OBA, F., TANAKA, I. Band structure diagram paths based on crystallography. *Computational Materials Science*. 2017, vol. 128, p. 140. https://doi.org/10.1016/j.commatsci.2016.10.015.